



## Hallucination-Specific structure-function associations in schizophrenia

Meighen M. Roes<sup>a,b</sup>, John Yin<sup>b,c</sup>, Laura Taylor<sup>b,c,†</sup>, Paul D. Metzrak<sup>d</sup>, Katie M. Lavigne<sup>e</sup>,  
Abhijit Chinchani<sup>b,c</sup>, Christine M. Tipper<sup>b,c</sup>, Todd S. Woodward<sup>b,c,\*</sup>

<sup>a</sup> Department of Psychology, University of British Columbia, Vancouver, BC, Canada

<sup>b</sup> BC Mental Health and Substance Use Services Research Institute, Provincial Health Services Authority, Vancouver, BC, Canada

<sup>c</sup> Department of Psychiatry, University of British Columbia, Vancouver, BC, Canada

<sup>d</sup> Department of Psychiatry, University of Calgary, Calgary, AB, Canada

<sup>e</sup> Department of Psychiatry, McGill University, Montreal, QC, Canada

### ARTICLE INFO

#### Keywords:

Neuroimaging  
Bipolar, hallucinations  
Multimodal  
fMRI  
Cortical thickness

### ABSTRACT

Combining structural (sMRI) and functional magnetic resonance imaging (fMRI) data in schizophrenia patients with and without auditory hallucinations (9 SZ\_AVH, 12 SZ\_nAVH), 18 patients with bipolar disorder, and 22 healthy controls, we examined whether cortical thinning was associated with abnormal activity in functional brain networks associated with auditory hallucinations. Language-task fMRI data were combined with mean cortical thickness values from 148 brain regions in a constrained principal component analysis (CPCA) to identify brain structure-function associations predictable from group differences. Two components emerged from the multimodal analysis. The “AVH component” highlighted an association of frontotemporal and cingulate thinning with altered brain activity characteristic of hallucinations among patients with AVH. In contrast, the “Bipolar component” distinguished bipolar patients from healthy controls and linked increased activity in the language network with cortical thinning in the left occipital-temporal lobe. Our findings add to a body of evidence of the biological underpinnings of hallucinations and illustrate a method for multimodal data analysis of structure-function associations in psychiatric illness.

### 1. Introduction

Auditory verbal hallucinations (AVH), the perceptions of external speech in the absence of any stimulus, are experienced by a majority of people with schizophrenia and an estimated 23%–31% of patients with bipolar disorder with psychotic features during the course of their illness (Smith et al., 2017; Waters et al., 2012). Schizophrenia and bipolar disorder share a genetic predisposition and considerable symptom overlap, but typically differ in phenomenology and severity of psychotic symptoms, including AVH. The common and distinct neural mechanisms underlying psychotic features in these disorders remain unclear (Baethge et al., 2005; Barrett et al., 2009; Bellack et al., 1989; Murray et al., 2004; Rosen et al., 2012, 1983). The current study aims to detect structure-function associations distinguishing hallucinating schizophrenia patients (SZ\_AVH) from non-hallucinating schizophrenia patients (SZ\_nAVH), non-hallucinating bipolar patients (BP), and healthy controls (HC).

Previous studies of the biological underpinnings of hallucinations

have mainly employed a single imaging modality, namely functional (fMRI) or structural (sMRI) magnetic resonance imaging (e.g., Gaser et al., 2004; Goldstein et al., 1999; Lawrie et al., 2002; Lennox et al., 2000; Neckelmann et al., 2006). sMRI investigations have consistently reported widespread changes in cortical gray matter (GM) in patients with schizophrenia and bipolar disorder relative to healthy controls (Bora et al., 2011; Chan et al., 2011; Ellison-Wright et al., 2008; Glahn et al., 2008; Hanford et al., 2016; Van Erp et al., 2018), with GM loss more extensive and profound in schizophrenia relative to bipolar disorder (Ivleva et al., 2013; Nenadic et al., 2015; Yuksel et al., 2012). AVH severity is most consistently associated with fronto-temporal GM loss (DeLisi et al., 2006; Kubera et al., 2014; Modinos et al., 2013; Mørch-Johnsen et al., 2017; Neckelmann et al., 2006; Padmanabhan et al., 2014; Palaniyappan et al., 2012), though associated GM reductions in the bilateral insula, anterior and posterior cingulate cortex (ACC and PCC), and other regions have also been reported (Allen et al., 2008; Martí-Bonmatí et al., 2007; Nenadic et al., 2010).

\* Corresponding author at: BC Mental Health and Substance Use Services Research Institute, Room 117, 3rd Floor, 938 W. 28th Avenue, Vancouver, B.C., Canada. V5Z 4H4.

E-mail address: [todd.woodward@ubc.ca](mailto:todd.woodward@ubc.ca) (T.S. Woodward).

† Deceased April 2016

<https://doi.org/10.1016/j.psychresns.2020.111171>

Received 31 January 2020; Received in revised form 15 August 2020; Accepted 19 August 2020

Available online 23 August 2020

0925-4927/ © 2020 Elsevier B.V. All rights reserved.

In fMRI research, AVH are associated with aberrant activity in frontotemporal regions related to speech perception and speech generation (Allen et al., 2012; Ćurčić-Blake et al., 2017; Dierks et al., 1999; Waters et al., 2012). Meta-analyses of symptom capture studies have concluded that the acute AVH state is characterized by frontotemporal hyper-activity (Allen et al., 2012; Jardri et al., 2011b). However, studies comparing patients with and without frequent AVH have reached mixed results regarding the direction of connectivity change associated with AVH traits. Resting-state symptom association studies have reported both hyper-activity (e.g., Chang et al., 2017; van Lutterveld et al., 2014) and hypo-activity (Clos et al., 2014; Sommer et al., 2012) in prefrontal and temporal regions among patients who experience AVH. In the task-based symptom association literature, degree of control over verbal processing may reconcile seemingly-contradictory findings, as SZ\_AVH patients tend to show reduced frontotemporal activity during controlled verbal processing or monitoring of inner speech (Curcic-Blake et al., 2013; McGuire et al., 1995; Shergill et al., 2003; Woodward et al., 2015) but increased activity during passive speech perception (Alderson-Day et al., 2017; Copolov et al., 2003; Lavigne et al., 2015; Lavigne and Woodward, 2018; Sanjuan et al., 2007; Zhang et al., 2008).

For example, in a previous task-based fMRI study, we found that SZ\_AVH showed increased activation of a language functional network and stronger co-deactivation of the default mode network during a passive speech-perception task compared to HC, BP, and SZ\_nAVH patients (Lavigne et al., 2015). This pattern was not observed in SZ\_AVH patients during silent thought generation (Lavigne et al., 2015), suggesting that exerting control over inner verbal thought processes decreases the severity or likelihood of hallucinations (Pynn and DeSouza, 2013).

While sMRI and fMRI approaches have advanced our understanding of the neurobiology of AVHs, single-modality studies cannot explore the interplay of anatomical and functional brain characteristics in the manifestation of psychotic symptoms. Methods combining multiple neuroimaging modalities, including diffusion tensor imaging with fMRI (Hermundstad et al., 2014; Koch et al., 2011; Schlosser et al., 2007), and sMRI with fMRI (Kubera et al., 2019; Schultz et al., 2012b) have begun to uncover potential structure-function relationships in brain pathologies related to psychosis (Liu et al., 2015). A general trend of these studies is that patients with schizophrenia exhibit different structure-function associations compared to HC (Calhoun and Sui, 2016; Schultz et al., 2012a; Sui et al., 2015, 2012). Studies are now needed to investigate the biological correlates of AVH from a multi-modal neuroimaging perspective. Further, psychiatric comparison groups (e.g., bipolar disorder) are needed to clarify the extent to which any structure-function abnormalities are specific to schizophrenia.

Previous explorations have mainly used ROI-based analyses (Benetti et al., 2015), focused on regions where functional and structural abnormalities coincide (Martí-Bonmatí et al., 2007), or studied resting-state connectivity (Kubera et al., 2019). However, functional connectivity - and as a consequence, observable structure-function associations - may be task-dependent, with brain structure differentially shaping spontaneous and task-evoked functional connectivity (e.g., Fornito et al., 2012; Hermundstad et al., 2013, 2014). To our knowledge, no study has investigated structure-function relationships underlying AVH with an fMRI task specifically designed to recruit AVH-related brain networks and a structural analysis not restricted to a limited number of pre-specified ROIs.

Using a novel application of constrained principal component analysis (CPCA; Hunter and Takane, 2002; Takane and Hunter, 2001; Takane and Shibayama, 1991) we investigated the structure-function relationships differentiating SZ\_AVH patients from SZ\_nAVH and control groups (BP, HC). We hypothesized that hyper-activation of the language network, and hyper-suppression of the default-mode network (DMN) during passive speech perception (Lavigne et al., 2015) would be associated with frontotemporal thinning among patients with AVH.

## 2. Methods

### 2.1. Participants

The sample consisted of a subset of participants of our previous fMRI-only study (Lavigne et al., 2015) who, in addition to functional imaging, had undergone sMRI scanning. Twenty-one patients (5 inpatients and 16 outpatients) with schizophrenia, 18 outpatients with bipolar disorder (BP; 11 males and 7 females, mean age = 38.9;  $SD = 11.3$ ), and 22 healthy controls (HC; 13 males and 9 females, mean age = 28.7;  $SD = 9.4$ ) were included. The schizophrenia sample was further divided into patients experiencing AVH (SZ\_AVH; 5 males, 4 females; mean age = 32.0;  $SD = 10.2$ ) and patients without AVH (SZ\_nAVH; 5 males, 7 females; mean age = 32.8;  $SD = 10.2$ ).

Patients' symptom severity over the past week was assessed using the Signs and Symptoms of Psychotic Illness scale (SSPI; see Supplementary Table S1 for means and group differences), (Liddle et al., 2002). Symptoms of mania in the past 48 h were evaluated using the Young Mania Rating Scale (Young et al., 1978). Patients with SSPI auditory hallucination ratings of 3 (definite hallucinations that do not pervasively influence thinking or behavior) or 4 (definite hallucinations that pervasively influence thinking and/or observable behavior) were included in the SZ\_AVH group. One BP patient reported hallucinations (rating of 2, visual hallucinations only). Of the 9 SZ\_AVH patients, 5 reported experiencing hallucinations in additional sensory modalities (tactile = 3; tactile & visual = 1; tactile & visual & olfactory = 1).

Among the non-hallucinating clinical groups, 10 of the SZ\_nAVH patients (auditory = 7, auditory and olfactory = 2; tactile = 1) and 7 BP patients (auditory = 1; visual = 3; visual and tactile = 1; auditory and visual and tactile and olfactory = 1) had a prior lifetime history of hallucinations. Age  $F(3, 57) = 3.29, p < .05$ , but not handedness,  $\chi^2(6, N = 61) = 4.2, p > .05$  nor gender,  $\chi^2(3, N = 61) = 1.27, p > .05$ , differed among groups. Post-hoc Tukey's HSD tests found BP participants to be significantly older than HC participants ( $p < .05$ ; see Table S2 of Supplementary Material). All participants met MRI compatibility criteria with experimental procedures approved by the University of British Columbia (UBC) and UBC Hospital Clinical Research Ethics Board. Participants received an honorarium and reimbursement for travel costs.

Exclusion criteria were: (1) a history of neurological disorder; (2) a diagnosis of substance abuse or dependence; and (3) a history of traumatic brain injury with cognitive sequelae or loss of consciousness greater than 5 min. Participants were excluded from the HC group if they had a personal or immediate family history of psychiatric illness. Patient diagnoses were confirmed using the Mini International Neuropsychiatric Interview (Hergueta et al., 1998) in concordance with Diagnostic and Statistical Manual of Mental Disorders—Fourth Edition. All participants had normal hearing and spoke English fluently.

### 2.2. Task

Participants were asked to either mentally generate (verbal thought generation; VTG) or listen to (speech perception; SP) a simple definition of an object (e.g., "Something you sit on"), after being presented with the object's name (e.g., chair) and its corresponding image (Fig. 2; Lavigne et al., 2015; Rapin et al., 2012). The conditions were presented in 15-trial blocks across two runs, totaling 30 trials per condition per participant.

### 2.3. Image acquisition

fMRI and sMRI data were acquired within 10 days of each other using a Philips Achieva 3.0 Tesla MR scanner at the UBC MRI Research center. Functional image volumes were collected using quasar dual gradients (maximum gradient amplitude of 80 mT/m and a maximum

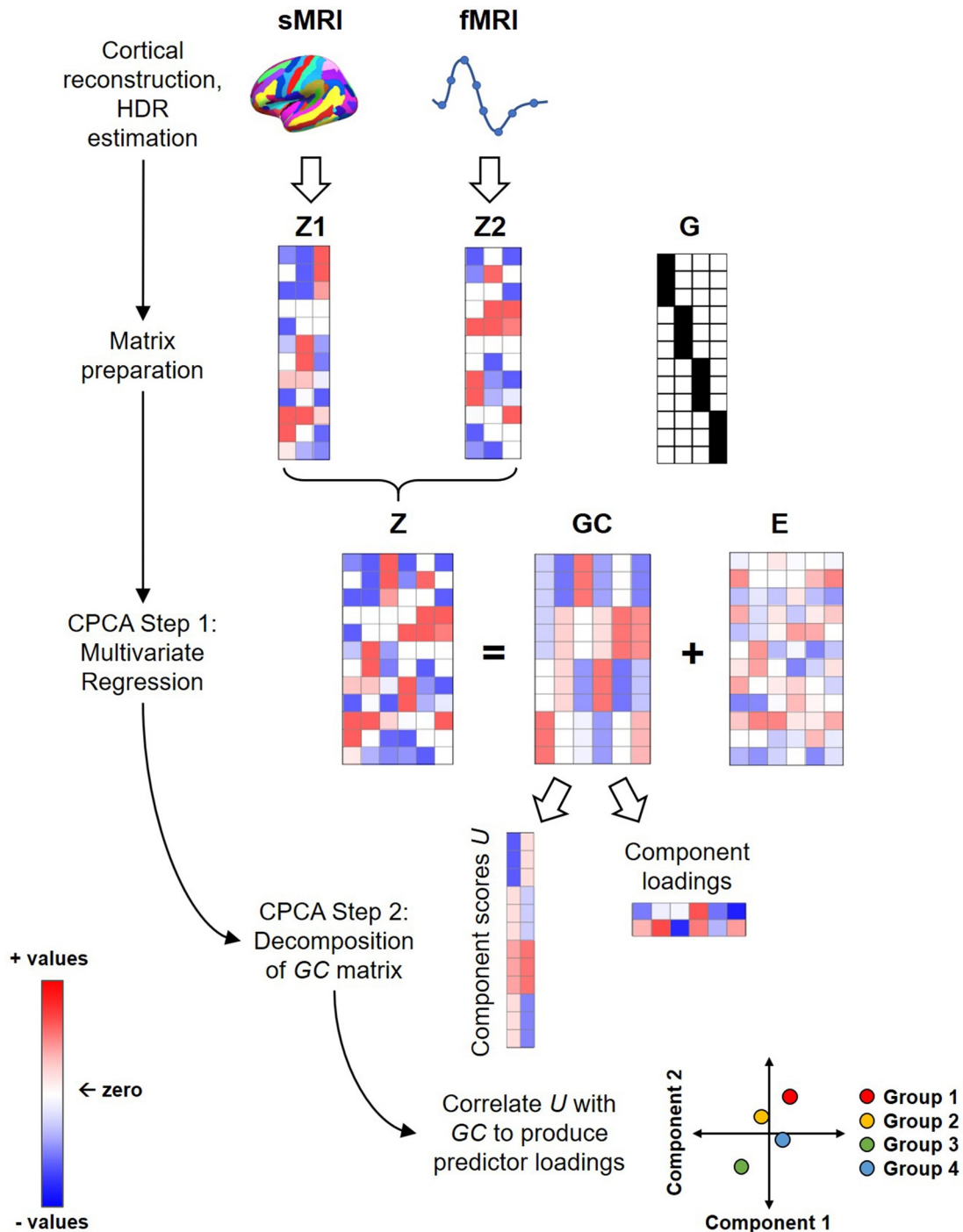


**Fig. 1.** Visual depiction of the data analysis pipeline. Cortical thickness (CT) values were obtained using cortical reconstruction, and sample-specific hemodynamic response (HDR) estimates for the language and DMN networks were obtained through an fMRI-CPCA analysis. In the matrix preparation phase, The CT and HDR values were represented in matrix form and combined into the data matrix  $Z$ . Group information was represented in the design matrix  $G$  through dummy-coding. In the regression step of multimodal CPCA, the multivariate data matrix  $Z$  was regressed onto  $G$ . Singular value decomposition was then applied to the  $GC$  matrix containing group-related variances in the multimodal data. Component loadings were computed to describe patterns of sMRI and fMRI variables related to group information. Finally, predictor weights were calculated to describe how group differences relate to the multimodal components.

slow rate of 200 mT/m/s) with a T2\*-weighted gradient echo spin pulse sequence (TR/TE 2500/30 ms, 90° flip angle, FOV 24 × 24 cm<sup>2</sup>, 80 × 80 matrix, 3.00 mm slice thickness, 1.00 mm gap size, 36 axial slices). 352 functional images were acquired over two runs of 450 s. Structural images were obtained using a three-dimensional T1-weighted SENSE-Head-8 sequence with 182 coronal slices (TR/TE 8.1/3.7 ms, FOV 256 × 200 × 182 mm<sup>3</sup>, scan duration 382 s)

#### 2.4. Data analysis

Fig. 1 presents an overview of our multimodal data analysis pipeline, through which CT values and HDR estimates were produced, represented in matrix form, and analyzed by multimodal CPCA in order to discover structure-function associations related to group information (SZ\_AVH, SZ\_nAVH, BP and HC).

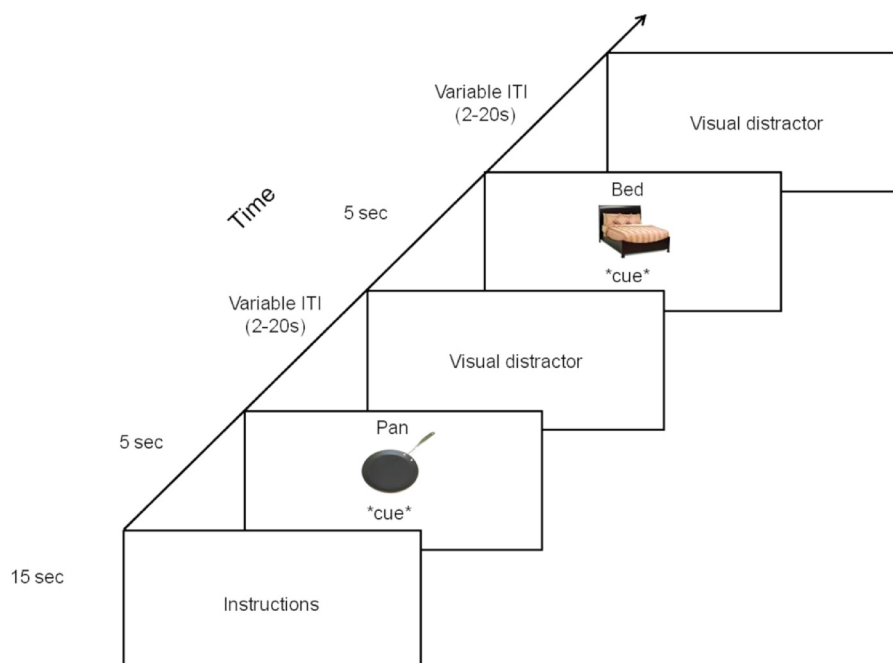


Fig. 2. Visual depiction of the experimental procedure. Two conditions, mentally generating a definition (verbal thought generation; VTG) or listening to a definition of a word (speech perception; SP) were cued with the phrases “something you...” or “listen...” during their respective condition-specific blocks. .

#### 2.4.1. Hemodynamic response estimation for language and default-mode networks

An fMRI-only analysis was conducted in order to obtain subject-, time- and condition-specific estimates of the language and default-mode networks' hemodynamic response (HDR) for use in the primary multimodal analysis. This re-analysis of a subset of participants from our previous unimodal study (Lavigne et al., 2015) was not conducted as a primary analysis, but rather in order to derive sample-specific estimates of our previously-published networks and their HDR shapes. Data analysis was carried out using constrained principal component analysis for fMRI (fMRI-CPCA) with orthogonal rotation (Hunter and Takane, 2002; Metzak et al., 2011, 2012; Takane and Hunter, 2001; Takane and Shibayama, 1991; Woodward et al., 2006, 2013), as described in the Supplementary Material. Briefly, fMRI-CPCA combines multivariate multiple regression with principal component analysis (PCA) of whole-brain activity to reveal independent sources of task-timing related BOLD activity (i.e., whole-brain functional networks). Component loadings for each voxel can be overlaid on a brain image and thresholded to visualize the regions contributing most strongly to each functional network. fMRI-CPCA also produces estimates of the engagement of the whole-brain functional networks for each combination of post-stimulus time bin, condition, and participant. These HDR estimates can be used to test group, condition, and time effects, and to verify a biologically plausible HDR shape. In the current study, these HDR estimate were retained as the fMRI variables included in our multimodal CPCA analysis.

#### 2.4.2. Cortical reconstruction for cortical thickness

We examined cortical thickness (CT) as our measure of GM integrity, as decreases in CT (not surface area) most strongly account for the reductions in cortical volume observed in schizophrenia and bipolar disorder (Rimol et al., 2012). CT has a genetic origin distinct from that of cortical surface area and may represent an endophenotype (Panizzon et al., 2009; Rimol et al., 2012; Winkler et al., 2010).

Cortical reconstruction for CT was conducted using the Freesurfer image analysis suite (version 5.3.0, <http://surfer.nmr.mgh.harvard.edu>; Dale et al., 1999; Destrieux et al., 2010; Fischl and Dale, 2000; Fischl et al., 1999). This process includes removal of non-brain tissue

from T1-weighted images, automated Talairach transformation, intensity normalization, tessellation of the gray/white matter boundary, automated topology correction, inflation, registration to a spherical atlas and automatic parcellation with identification of 74 distinct gyral and sulcal regions per hemisphere (Destrieux et al., 2010). CT was calculated as the distance between the gray and white matter boundaries at each vertex. Mean CT was automatically calculated for each region, and the final cortical reconstruction was visually inspected for accuracy. One schizophrenia subject was excluded from analysis due to poor image quality. Due to the potential confound between age and cortical thinning, CT in all regions was regressed onto age, and the residuals were used in all subsequent analyses.

#### 2.4.3. Multimodal structure-function analysis

Comprehensive theorems and proofs behind CPCA as a general methodology have been published previously (Hunter and Takane, 2002; Takane and Hunter, 2001; Takane and Shibayama, 1991). Briefly, CPCA uses multiple linear regression to constrain variance in an observed data matrix  $Z$  (here, multimodal sMRI-fMRI data) to that which is predictable from a design matrix  $G$  (group information); next, the predicted scores from the regression are submitted to singular value decomposition (SVD) to discover patterns of intercorrelation in the data that are related to the design matrix  $G$ . The current study applies CPCA methodology to a multimodal analysis to uncover structure-function associations related to group differences present in the data (Hunter and Takane, 2002; Lavigne et al., 2013; Luk et al., 2018).

To prepare for our novel multimodal CPCA analysis, the sMRI-fMRI data were arranged into a 2-dimensional data matrix,  $Z$ . The rows of  $Z$  represented the 61 participants, and the columns of  $Z$  contained the subject-specific network HDR estimates, and the CT values obtained during the HDR estimation and cortical reconstruction analyses, respectively. Thus, to form  $Z$ , two matrices  $Z1$  and  $Z2$  were horizontally concatenated with  $Z1$  (a  $61 \times 148$  matrix) containing standardized mean CT values for the 148 gyral and sulcal regions and  $Z2$  (a  $61 \times 36$  matrix) containing 36 HDR estimates from the fMRI-only analysis [9 post-stimulus time bins \* 2 conditions (VTG and SP) \* 2 networks (language network and DMN)]. Therefore, with 61 participants and a

total of 184 structural and functional variables, the full data matrix  $Z$  had dimensions of  $61 \times 184$ .

The design matrix  $G$  was a  $61 \times 4$  matrix, with each row corresponding to each participant who forms a row in  $Z$ . Group information (HC, BP, SZ\_nAVH and SZ\_AVH) was encoded in the columns of  $G$  by means of dummy coding, wherein membership in a particular group is coded with a value of 1, and non-membership in the group is coded with a value of 0 (Cohen et al., 2013). Dummy coding incorporates the categorical variable of group membership into the multivariate regression step of CPCA.

In the multivariate least squares regression analysis step of CPCA,  $Z$  is regressed onto  $G$  to partition the total variance into that which can be explained by  $G$  (here, group information) and that which cannot (matrix  $E$ );  $Z = GC + E$ . In the regression model,  $C$  is a matrix of beta weights,  $C = (G'G)^{-1}G'Z$ , and  $G*C = Z'$ , where  $Z'$  is a matrix of predicted scores, one for each variable in  $Z$ . In the current multimodal CPCA analysis,  $GC$  contains predicted scores for each subject's structural and functional data, as predicted by group information (i.e., whether the participant is HC, BP, H\_SZ, NH\_SZ).

In the second step of CPCA, SVD (Eckart and Young, 1936) is applied to the  $GC$  matrix to extract the dominant patterns of intercorrelation in the multimodal data, constrained to variance predictable from the group memberships specified in  $G$ ;  $SVD(GC) = [U, D, V']$ . This decomposition yields a) the right singular vectors ( $V$ ), b) the diagonal matrix of singular values ( $D$ ), and c) the left singular vectors ( $U$ ). A scree plot of the singular values is examined to determine the number of multimodal components to retain (Cattell, 1966). Because group membership (coded in  $G$ ) is used as a set of predictor variables, a decomposition of  $GC$  produces a multidimensional solution, each with component loadings that describe patterns optimized to be predictable from group membership. Component loadings are computed by rescaling the right singular vectors;  $VD/\sqrt{(n-1)}$ . Component loadings represent the contribution of each variable (e.g., CT in region 'X' or DMN activity at time bin 'Y') to each  $GC$  component, and they therefore hold the key to identifying structure-function associations related to group information. Component loadings for structural variables can be overlaid onto a brain atlas to visualize patterns of cortical thinning/thickening most strongly contributing to each component. Where both functional (HDR) and structural (CT) variables represent the dominant loadings for a component, one can conclude that a structure-function relationship characterizes that component.

Next, predictor loadings are calculated by correlating component scores with the design matrix. When interpreted together with component loadings, predictor loadings indicate how  $G$  variables (group membership) relate to each  $GC$  component; they are therefore the key to understanding how group differences relate to structure-function associations. For example, predictor loadings nearing the contrasting values of  $-1$  and  $1$  for two groups would indicate that the contrast between those particular groups accounts for most of the variance in that component. We were therefore particularly interested in characterizing (by interpreting component loadings) any multimodal components where predictor loadings indicated that the contrast between SZ\_AVH and other groups accounted for most of the component's variance.

#### 2.4.4. Visualization and characterization of multimodal components

To better understand the group differences highlighted by our multimodal analysis, independent samples  $t$ -tests were conducted on mean age-corrected CTs. The top 5% of each component's loadings were tested in this Regions-of-Interest (ROI) analysis (Supplementary Tables S3 and S4). Brain regions with a significance of  $p < .005$  were overlaid onto a structural atlas and ranked according to  $t$ -values (Figure 4 and 5, Tables 1 and 2). Similar  $t$ -tests were conducted comparing functional data (HDR estimates) for the dominant 10% of component loadings (Supplementary Tables S3 and S5).

#### 2.4.5. Permutation testing of the variance accounted for by group information

Permutation testing investigated whether group information accounted for variance in the multimodal data above chance level. A 10,000 iteration bootstrapping procedure was run whereby  $G$  (dummy coded for group: HC, BP, SZ\_nAVH and SZ\_AVH) predicted random permutations of  $Z$  (CT and HDR measures). This process builds a null distribution of variance in  $Z$  accounted for by  $G$ . A  $p$ -value is estimated as the proportion of times the permuted variance exceeds the observed variance.

### 3. Results

#### 3.1. Hemodynamic response estimation for language and default-mode networks

As anticipated, the spatial and temporal characteristics of the DMN and language networks (See Fig. 3) closely replicated those obtained in our original unimodal study (Lavigne et al., 2015). The purpose of the fMRI-only analysis was solely to obtain sample-specific HDR estimates on the same sample for which we have structural data, for use in the multimodal analysis, and this replication is not a novel finding; therefore, detailed results of the current study's fMRI-only analysis are presented in Supplementary Materials (see Supplementary Tables S6-S9 and Supplementary Figure S1).

#### 3.2. Multimodal structure-function analysis

After inspection of the scree plot obtained from SVD of the multimodal dataset, two components were retained (Cattell, 1966; Cattell and Vogelmann, 1977), accounting for 67.3% and 18.8% of the variance in sMRI-fMRI data predictable from group information, respectively. Permutation testing found that the proportion of variance in the multimodal data accounted for by group information (9.00%) was statistically significant ( $p = .001$ ).

From the graph of the predictor loadings (Fig. 6) it is evident that component 1 best describes the differences between SZ\_AVH and other patients, whereas component 2 describes the difference between BP and HC. For ease of reference, these multimodal components will be hereafter be referred to as the "AVH" and "Bipolar" components.

#### 3.3. Visualization and characterization of multimodal components

The sMRI and fMRI component loadings for the multimodal analysis are depicted in Figs. 4 and 5 and Tables 1 and 2. To facilitate interpretation, structural and functional component loadings are presented separately but retain their own scale. For the "AVH" component,  $t$ -tests revealed that, among the regions representing the top 10% of sMRI component loadings, six were significantly thinner in SZ\_AVH compared to other psychiatric groups: the right orbital gyrus, the triangular part of the right inferior frontal gyrus, the left and right middle frontal gyrus, the left dorsal PCC, and the right middle temporal gyrus (see Table 1). Aspects of network recruitment during the SP condition dominated the functional loadings for this component (language time bin 4 [peak activation] and 9 [post-activation suppression] and DMN time bins 5 and 6 [return from suppression]), indicating that an interplay between the language network and DMN characterized the functional contribution to this multimodal component (See Table 1).  $t$ -tests comparing HDR estimates between SZ\_AVH and other patient groups did not reach significance. Interpreting the multimodal component loadings and predictor loading together, SZ\_AVH patients were distinguished from non-AVH (BP and SZ\_nAVH) patients by an association of fronto-temporal and PCC thinning with language network hyperactivity and DMN hyper-suppression during passive speech perception.

For the "Bipolar" component,  $t$ -tests on the structural data comparing BP to HC revealed that, among the regions representing the top

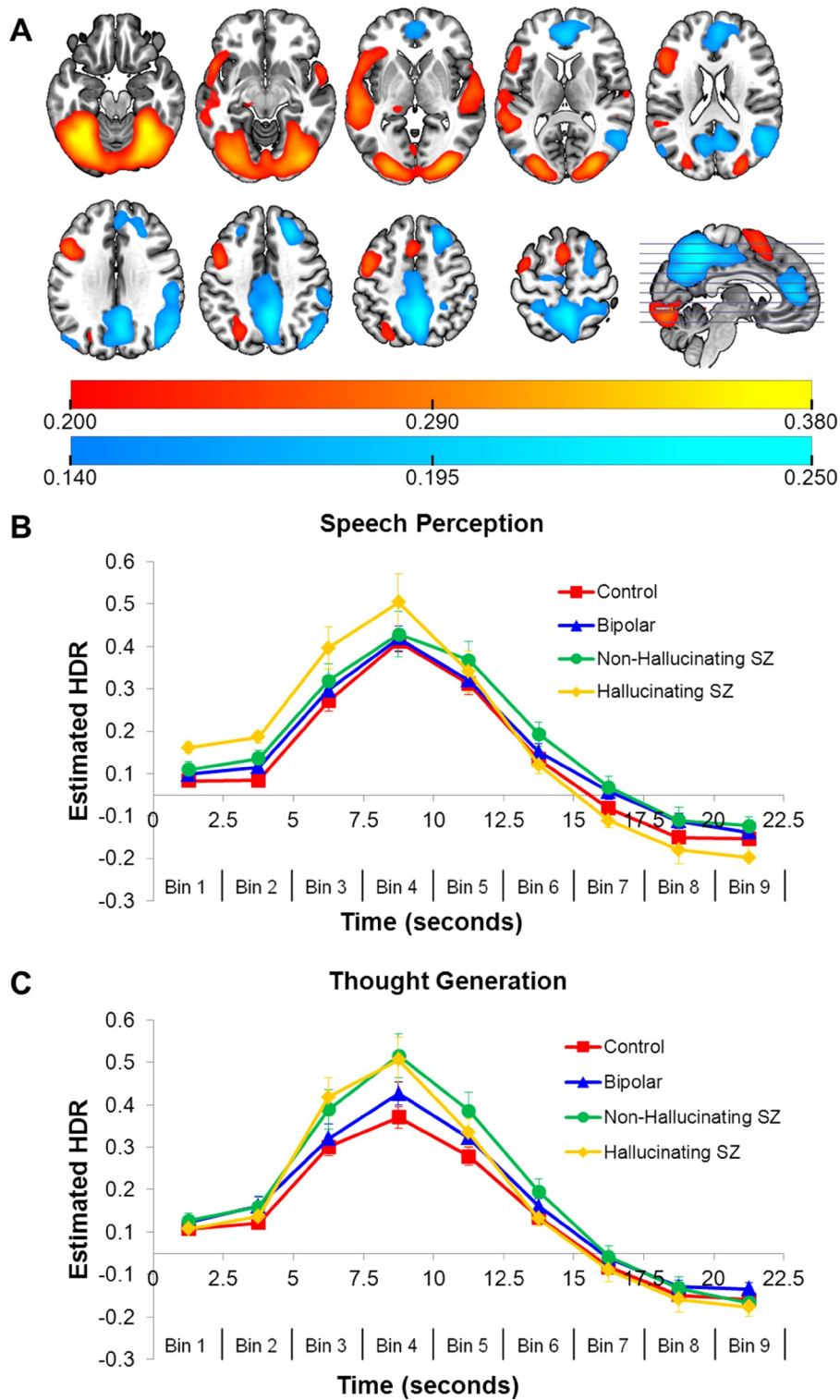


**Fig. 3.** Results of unimodal fMRI-CPA analysis. (A) Dominant 10% of component loadings for the Language functional network (orange/yellow, threshold = 0.20, max = 0.38, no negative loadings passed threshold) and the default mode network (DMN; blue, threshold = 0.14, max = 0.25, min = -0.25). Axial slices represent Montreal Neurological Institute Z-axis coordinates -20, -10, 0, 10, 20, 30, 40, 50, 60. (B and C) Mean predictor weights for speech perception (B) and verbal thought generation (C) averaged over DMN and Language networks, plotted over peristimulus time. Error bars are SEs; HDR = estimated hemodynamic response.

10% of loadings, two brain regions – the left middle temporal gyrus and anterior occipital sulcus– were significantly thinner in BP patients (see Fig. 5 and Table 2). BP participants had significantly greater Language network activity relative to HC in both the SP and VTG conditions at time bins 5 and 6, when hemodynamic activity was returning to baseline. Taking these findings together, an association of left temporal-

occipital cortical thinning with increased/prolonged language network activation distinguished BP from HC participants.

**4. Discussion**

Combining structural (sMRI) and functional magnetic resonance

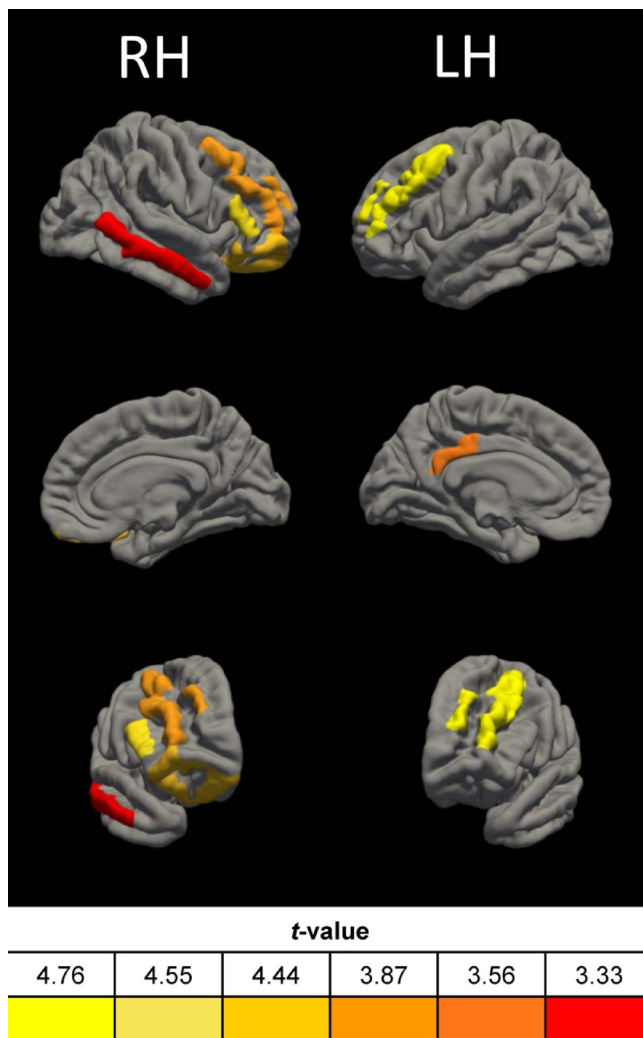


**Fig. 4.** Dominant cortical thickness and hemodynamic response (HDR) component loadings for the “AVH” multimodal component of strongly-loading brain regions that were thinner in hallucinating schizophrenia patients as compared to non-hallucinating schizophrenia patients ( $p < .005$ ). Images from top to bottom indicate a lateral, medial, and fronto-oblique view of the brain respectively. Corresponding regions are presented on [Table 1](#) and color-coded according to  $t$ -value. RH = Right hemisphere. LH = Left hemisphere.

imaging (fMRI) data in schizophrenia patients with and without AVH, patients with bipolar disorder, and healthy controls, we examined whether cortical thinning was associated with abnormal activity in functional brain networks associated with AVH. Functional and structural MRI data were entered into a single data set, and CPCA was used to discover constructs underlying associations between them. Language task fMRI data were combined with mean CT values from 148 brain regions in a constrained principal component analysis (CPCA) to identify brain structure-function associations predictable from group differences. Two components emerged from the multimodal analysis. The “AVH component” highlighted an association of frontotemporal and cingulate thinning with altered brain activity characteristic of hallucinations among patients with AVH. The “Bipolar component” differentiated bipolar patients from healthy controls and associated hyperactivity in the language network with cortical thinning in the left occipital-temporal lobe.

The “AVH component” described an association between frontotemporal and PCC thinning with anti-correlating DMN and language network activity during passive speech perception among patients with AVH. GM reductions in frontotemporal regions have been found in

**Table 1**

Dominant cortical thickness (sMRI) and hemodynamic response (fMRI) component loadings for the “AVH” multimodal component, presented alongside  $t$ - and  $p$ - values for contrasts of the hallucinating and nonhallucinating patient groups on raw sMRI and fMRI measures (for the full set of results see Supplementary Material Tables S4 and S5).

Brain region	Component Loading	t-value	p
Left middle frontal gyrus	0.490	4.76	<0.001
Right triangular part of inferior frontal gyrus	0.528	4.55	<0.001
Right orbital gyrus	0.498	4.44	<0.001
Right middle frontal gyrus	0.494	3.87	0.001
Posterior-dorsal part of the left cingulate gyrus	0.460	3.56	0.002
Right middle temporal gyrus	0.437	3.33	0.004
Predictor Weight	Component Loading	t-value	p
Language SP time bin 4	0.304	-1.55	0.137
Language SP time bin 9	0.261	-1.49	0.153
DMN SP time bin 5	0.228	-0.80	0.433
DMN SP time bin 6	0.221	-0.65	0.521

Note: Dominant cortical thickness and hemodynamic response (HDR) component loadings for the “AVH” multimodal component of strongly-loading brain regions that were thinner in hallucinating schizophrenia patients as compared to non-hallucinating schizophrenia patients ( $p < .005$ ) and dominant HDR component loadings for the “AVH” component. Corresponding brain regions are shown on [Fig. 4](#). SP = Speech perception condition.

**Table 2**

Dominant cortical thickness (sMRI) and hemodynamic response (fMRI) component loadings for the “Bipolar” multimodal component, presented alongside  $t$ - and  $p$ - values for contrasts of the bipolar and healthy control groups on raw sMRI and fMRI measures (for the full set of results see Supplementary Material Tables S4 and S5).

Brain region	Component Loading	t-value	p
Left middle temporal gyrus	0.239	3.404	0.002
Left anterior occipital sulcus and pre-occipital notch	0.376	3.232	0.002
Predictor Weight	Component Loading	t-value	p
Language VTG time bin 6	0.402	-2.825	0.007
Language VTG time bin 5	0.377	-3.347	0.002
Language SP time bin 6	0.310	-2.136	0.034
Language SP time bin 7	0.251	-1.343	0.189

Note: Dominant cortical thickness and hemodynamic response (HDR) component loadings for the “Bipolar” multimodal component of strongly-loading brain regions that were thinner in bipolar patients as compared to healthy controls ( $p < .005$ ) and dominant HDR component loadings for the “Bipolar” component. Corresponding brain regions are shown on [Fig. 4](#). SP = Speech perception condition. VTG = Verbal Thought Generation Condition.

many studies examining the anatomy of schizophrenia patients who experience AVH ([Allen et al., 2008](#); [DeLisi et al., 2006](#); [Garcia-Marti et al., 2012](#); [Kubera et al., 2014](#); [Modinos et al., 2013](#); [Nenadic et al., 2010](#); [Palaniyappan et al., 2012](#)), whereas associations of PCC abnormalities with AVH have been less consistent ([Calabrese et al., 2008](#); [Martí-Bonmatí et al., 2007](#); [Wang et al., 2007](#)). The addition of PCC thinning to the “AVH” component was therefore not hypothesized, but is interesting considering its role as a key node of the DMN ([Buckner et al., 2008](#)). The posterior DMN, including the PCC, is associated with semantic and memory functions including autobiographical memory and awareness of self-initiated actions such as speaking ([Jardri et al., 2011a](#); [Spaniel et al., 2016](#); [Spreng et al., 2009](#)). The observed hyper-activation of the language network and hyper-suppression of the DMN could reflect an abnormal silencing of internally-focused DMN activity, and a shift toward processing of speech or

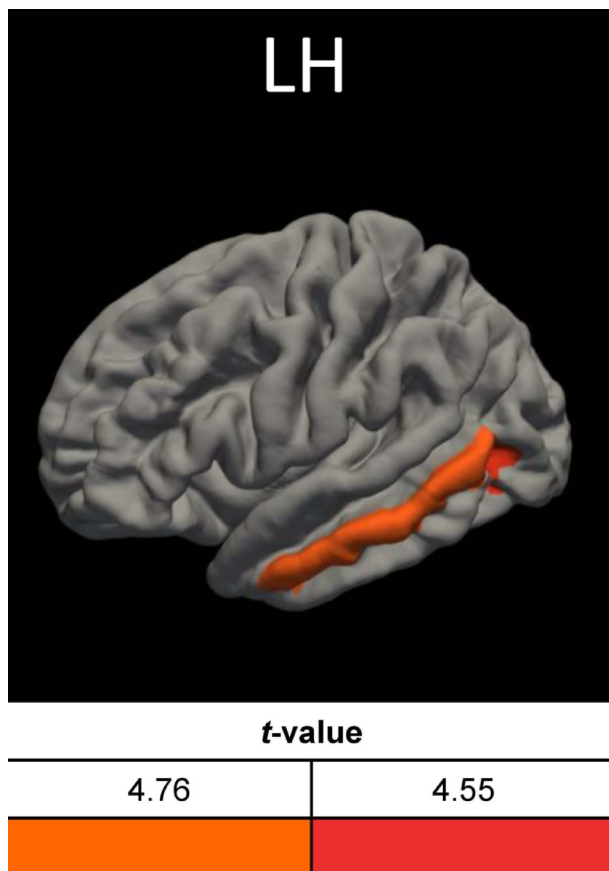


**Fig. 5.** Dominant cortical thickness and hemodynamic response (HDR) component loadings for the “Bipolar” multimodal component of strongly-loading brain regions that were thinner in bipolar patients as compared to healthy controls ( $p < .005$ ). These regions were limited to the left hemisphere (LH). Corresponding region labels are presented on Table 2 and color-coded according to  $t$ -value. .

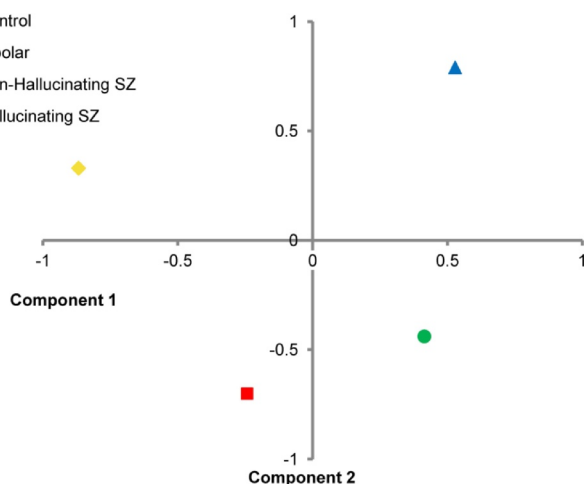


**Fig. 6.** Predictor weights resulting from multimodal CPCA analysis of cortical thickness and hemodynamic response variables. Component 1 (AVH) distinguished hallucinating schizophrenia patients from non-hallucinating patients. Component 2 (Bipolar) distinguished bipolar patients from healthy controls.

sensory percepts, during AVH-like states. Spontaneous AVH have been associated with withdrawal of the DMN and hyperactivity of the insula, frontotemporal and auditory association cortices (Jardri et al., 2013). Thus, the current study links structural abnormalities in frontotemporal

and PCC regions with altered brain activity characteristic of hallucinations.

It is notable that many regions that have been found to be thinner in AVH patients, such as the left STG (Mørch-Johnsen et al., 2017), did not load strongly onto the AVH component in the current study. Whereas thinning in the left STG and other cortical regions may be important for hallucinations, the right STG and other regions highlighted by our analysis appear to be more strongly associated with group differences in brain activity during passive speech perception. The strength of the multimodal CPCA approach lies precisely in its ability to examine the relevance of structural abnormalities to functional alterations in diagnostic groups.

On the surface, the increased functional connectivity we report appears inconsistent with the fronto-temporal disconnection hypothesis of AVH, which holds that a functional disconnection between frontal and temporal regions results in autonomous network activation and aberrant perceptions (David, 1994; Woodward and Menon, 2013). Furthermore, resting-state studies have generally found that schizophrenia patients and at-risk groups have reduced spontaneous anticorrelations between the DMN and task-related brain regions, a pattern that associates with hallucination severity (Manoliu et al., 2014; Supekar et al., 2019; Whitfield-Gabrieli et al., 2009; Wotruba et al., 2013). Such seemingly-contradictory findings may be explained by the highly task-dependent nature of inter- and intra-network functional connectivity and structure-function associations (Fornito et al., 2012; Hermundstad et al., 2014). Structure-function associations related to AVH are likely to be specific to particular cognitive states, with resting state structure-function associations expected to better reflect trait-rather than state- markers of hallucination proneness (Kubera et al., 2019). Future multimodal studies using symptom-relevant fMRI tasks (e.g., symptom capture studies) will help to further disentangle the complex structure-function interrelationships characterizing AVH.

The “Bipolar” multimodal component distinguished BP from HC participants and linked left occipito-temporal lobe thinning with increased activation of the language functional network. That this relationship was most characteristic of the bipolar group may reflect disease progression specific to this disorder, as reductions in temporal lobe GM have been found to correlate with functional decline in bipolar disorder but not schizophrenia (Qiu et al., 2013), and with intellectual decline and the number of intervening mood episodes in a 4-year prospective longitudinal study (Moorhead et al., 2007).

4.1. Limitations and future directions

The correlational and cross-sectional nature of this analysis precludes any conclusion as to the directionality of the reported structure-function associations. Short term state-dependent changes are known to occur in cortical GM, including the prefrontal cortex, temporal cortex, and PCC (Holzel et al., 2011; Seminowicz et al., 2013). Cortical thinning could therefore represent a state-dependent change, or may instead reflect traits such as treatment responsiveness, as longitudinal studies have found associations between frontotemporal GM integrity and treatment response in psychotic patients (Mitelman et al., 2009; Palaniyappan et al., 2013). Alternatively, AVH may covary with CT due to third variables such as psychological distress, in line with evidence that CBT and mindfulness increase bilateral dorsolateral PFC and PCC GM respectively (Holzel et al., 2011; Seminowicz et al., 2013). Longitudinal multimodal neuroimaging studies will be helpful in clarifying the directionality of structure-function associations in AVH.

We acknowledge the limitations of small sample sizes and the resultant risks of Type II error and over-fitting based on limited data, as well as the use of self-report to verify active engagement in the verbal thought generation condition. Further, we cannot definitively rule out the possibility that non-AVH differences between groups (e.g., delusions) could contribute to the present results, although our task was specifically designed to recruit AVH-associated functional networks.

Further, bipolar disorder subtypes were not tracked, and several studies have found significant differences between bipolar I and II in CT and risk for AVH, suggesting structure-function associations may differ across subtypes of the disorder (Elvsåshagen et al., 2013; Lyoo et al., 2006; Rimol et al., 2010). Finally, effects of medication and illness chronicity were not assessed.

Despite these limitations, the current study has the significant advantage of using a whole-brain analysis of multimodal data, without constraining analysis *a priori* to ROIs.

#### 4.2. Conclusion

Among patients with auditory hallucinations, altered brain activity characteristic of hallucinations was associated with frontotemporal and cingulate thinning. This study demonstrates a novel, data-driven method for combining structural and functional neuroimaging data for discovering biomarkers of psychotic illness.

#### Declaration of Competing Interest

The authors declare no conflicts of interest.

#### Acknowledgement

This project was supported through a scholar award to T.S.W. from the Michael Smith Foundation for Health Research, a New Investigator Award from the Canadian Institutes of Health Research, and a Canadian Institutes of Health Research operating grant (MOP-64431). We thank the UBC MRI Research center and John Païement for their assistance. The authors declare no conflicts of interest in relation to the subject of this study.

#### Supplementary materials

Supplementary material associated with this article can be found, in the online version, at [doi:10.1016/j.psychres.2020.111171](https://doi.org/10.1016/j.psychres.2020.111171).

#### References

Alderson-Day, B., Lima, C.F., Evans, S., Krishnan, S., Shanmugalingam, P., Fernyhough, C., Scott, S.K., 2017. Distinct processing of ambiguous speech in people with non-clinical auditory verbal hallucinations. *Brain* 140, 2475–2489. <https://doi.org/10.1093/brain/awx206>.

Allen, P., Laroi, F., McGuire, P.K., Aleman, A., 2008. The hallucinating brain: a review of structural and functional neuroimaging studies of hallucinations. *Neurosci. Biobehav. Rev.* 32, 175–191. <https://doi.org/10.1016/j.neubiorev.2007.07.012>.

Allen, P., Modinos, G., Hubl, D., Shields, G., Cachia, A., Jardri, R., Thomas, P., Woodward, T., Sholtb, P., Plaze, M., Hoffman, R., 2012. Neuroimaging auditory hallucinations in schizophrenia: from neuroanatomy to neurochemistry and beyond. *Schizophr. Bull.* 38, 695–703. <https://doi.org/10.1093/schbul/sbs066>.

Baethge, C., Baldessarini, R.J., Freudenthal, K., Streeruwitz, A., Bauer, M., Bschor, T., 2005. Hallucinations in bipolar disorder: characteristics and comparison to unipolar depression and schizophrenia. *Bipolar. Disord.* 7, 136–145. <https://doi.org/10.1111/j.1399-5618.2004.00175.x>.

Barrett, S.L., Mulholland, C.C., Cooper, S.J., Rushe, T.M., 2009. Patterns of neurocognitive impairment in first-episode bipolar disorder and schizophrenia. *Br. J. Psychiatry.* 195, 67–72. <https://doi.org/10.1192/bjp.bp.108.054874>.

Bellack, A.S., Morrison, R.L., Mueser, K.T., Wade, J., 1989. Social competence in schizophrenia: bipolar disorder, and negative and non-negative schizophrenia. *Schizophr. Res.* 2, 391–401. [https://doi.org/10.1016/0920-9964\(89\)90032-7](https://doi.org/10.1016/0920-9964(89)90032-7).

Benetti, S., Petterson-Yeo, W., Allen, P., Catani, M., Williams, S., Barsaglini, A., Kambeitz-Ilanckovic, L.M., McGuire, P., Mechelli, A., 2015. Auditory verbal hallucinations and brain dysconnectivity in the perisylvian language network: a multimodal investigation. *Schizophr. Bull.* 41, 192–200. <https://doi.org/10.1093/schbul/sbt172>.

Bora, E., Fornito, A., Radua, J., Walterfang, M., Seal, M., Wood, S.J., Yucel, M., Velakoulis, D., Pantelis, C., 2011. Neuroanatomical abnormalities in schizophrenia: a multimodal voxelwise meta-analysis and meta-regression analysis. *Schizophr. Res.* 127, 46–57. <https://doi.org/10.1016/j.schres.2010.12.020>.

Buckner, R.L., Andrews-Hanna, J.R., Schacter, D.L., 2008. The brain's default network: anatomy, function, and relevance to disease. *Ann. N. Y. Acad. Sci.* 1124, 1–38. <https://doi.org/10.1196/annals.1440.011>.

Calabrese, D.R., Wang, L., Harms, M.P., Ratnanather, J.T., Barch, D.M., Cloninger, C.R., Thompson, P.A., Miller, M.I., Csernansky, J.G., 2008. Cingulate gyrus neuroanatomy

in schizophrenia subjects and their non-psychotic siblings. *Schizophr. Res.* 104, 61–70. <https://doi.org/10.1016/j.schres.2008.06.014>.

Calhoun, V.D., Sui, J., 2016. Multimodal fusion of brain imaging data: a key to finding the missing link(s) in complex mental illness. *Biol. Psychiatry. Cogn. Neurosci. Neuroimaging* 1, 230–244. <https://doi.org/10.1016/j.bpsc.2015.12.005>.

Cattell, R.B., 1966. The Scree Test For The Number Of Factors. *Multivariate Behav. Res.* 1, 245–276. <https://doi.org/10.1207/s15327906mbr0102.10>.

Cattell, R.B., Vogelman, S., 1977. A comprehensive trial of the scree and KG criteria for determining the number of factors. *Multivariate. Behav. Res.* 12, 289–325.

Chan, R.C., Di, X., McAlonan, G.M., Gong, Q.Y., 2011. Brain anatomical abnormalities in high-risk individuals, first-episode, and chronic schizophrenia: an activation likelihood estimation meta-analysis of illness progression. *Schizophr. Bull.* 37, 177–188. <https://doi.org/10.1093/schbul/sbp073>.

Chang, X., Collin, G., Xi, Y., Cui, L., Scholtens, L.H., Sommer, I.E., Wang, H., Yin, H., Kahn, R.S., van den Heuvel, M.P., 2017. Resting-state functional connectivity in medication-naïve schizophrenia patients with and without auditory verbal hallucinations: a preliminary report. *Schizophr. Res.* 188, 75–81. <https://doi.org/10.1016/j.schres.2017.01.024>.

Clos, M., Diederer, K.M., Meijering, A.L., Sommer, I.E., Eickhoff, S.B., 2014. Aberrant connectivity of areas for decoding degraded speech in patients with auditory verbal hallucinations. *Brain Struct. Funct.* 219, 581–594. <https://doi.org/10.1007/s00429-013-0519-5>.

Cohen, J., Cohen, P., West, S.G., Aiken, L.S., 2013. *Applied Multiple Regression/Correlation Analysis For the Behavioral Sciences*. Routledge.

Copolov, D.L., Seal, M.L., Maruff, P., Ulusoy, R., Wong, M.T., Tochon-Danguy, H.J., Egan, G.F., 2003. Cortical activation associated with the experience of auditory hallucinations and perception of human speech in schizophrenia: a PET correlation study. *Psychiatry. Res.* 122, 139–152. [https://doi.org/10.1016/s0925-4927\(02\)00121-x](https://doi.org/10.1016/s0925-4927(02)00121-x).

Čurčić-Blake, B., Ford, J.M., Hubl, D., Orlov, N.D., Sommer, I.E., Waters, F., Allen, P., Jardri, R., Woodruff, P.W., David, O., Muler, C., Woodward, T.S., Aleman, A., 2017. Interaction of language, auditory and memory brain networks in auditory verbal hallucinations. *Prog. Neurobiol.* 148, 1–20. <https://doi.org/10.1016/j.pneurobio.2016.11.002>.

Curcic-Blake, B., Liemburg, E., Vercammen, A., Swart, M., Kneegting, H., Buggeman, R., Aleman, A., 2013. When Broca goes uninformed: reduced information flow to Broca's area in schizophrenia patients with auditory hallucinations. *Schizophr. Bull.* 39, 1087–1095. <https://doi.org/10.1093/schbul/sbs107>.

Dale, A.M., Fischl, B., Sereno, M.L., 1999. Cortical surface-based analysis. I. Segmentation and surface reconstruction. *Neuroimage* 9, 179–194. <https://doi.org/10.1006/nimg.1998.0395>.

David, A.S., 1994. Dysmodularity: a neurocognitive model for schizophrenia. *Schizophr. Bull.* 20, 249–255. <https://doi.org/10.1093/schbul/20.2.249>.

DeLisi, L.E., Szulc, K.U., Bertisch, H.C., Majcher, M., Brown, K., 2006. Understanding structural brain changes in schizophrenia. *Dialogues Clin. Neurosci.* 8, 71–78.

Destrieux, C., Fischl, B., Dale, A., Hagren, E., 2010. Automatic parcellation of human cortical gyri and sulci using standard anatomical nomenclature. *Neuroimage* 53, 1–15.

Dierks, T., Linden, D.E., Jandl, M., Formisano, E., Goebel, R., Lanfermann, H., Singer, W., 1999. Activation of Heschl's gyrus during auditory hallucinations. *Neuron* 22, 615–621. [https://doi.org/10.1016/s0896-6273\(00\)80715-1](https://doi.org/10.1016/s0896-6273(00)80715-1).

Eckart, C., Young, G., 1936. The approximation of one matrix by another of lower rank. *Psychometrika* 1, 211–218.

Ellison-Wright, I., Glahn, D.C., Laird, A.R., Thelen, S.M., Bullmore, E., 2008. The anatomy of first-episode and chronic schizophrenia: an anatomical likelihood estimation meta-analysis. *Am. J. Psychiatry* 165, 1015–1023. <https://doi.org/10.1176/appi.ajp.2008.07101562>.

Elvsåshagen, T., Westlye, L.T., Bøen, E., Hol, P.K., Andreassen, O.A., Boye, B., Malt, U.F., 2013. Bipolar II disorder is associated with thinning of prefrontal and temporal cortices involved in affect regulation. *Bipolar Disord.* 15, 855–864.

Fischl, B., Dale, A.M., 2000. Measuring the thickness of the human cerebral cortex from magnetic resonance images. *Proc. Natl. Acad. Sci. U. S. A.* 97, 11050–11055. <https://doi.org/10.1073/pnas.200033797>.

Fischl, B., Sereno, M.L., Tootell, R.B., Dale, A.M., 1999. High-resolution intersubject averaging and a coordinate system for the cortical surface. *Hum. Brain Mapp.* 8, 272–284. [https://doi.org/10.1002/\(sici\)1097-0193\(1999\)8:4<272::aid-hbm10>3.0.co;2-4](https://doi.org/10.1002/(sici)1097-0193(1999)8:4<272::aid-hbm10>3.0.co;2-4).

Fornito, A., Harrison, B.J., Zalesky, A., Simons, J.S., 2012. Competitive and cooperative dynamics of large-scale brain functional networks supporting recollection. *Proc. Natl. Acad. Sci. U. S. A.* 109, 12788–12793. <https://doi.org/10.1073/pnas.1204185109>.

Garcia-Marti, G., Aguilar, E.J., Marti-Bonmati, L., Escarti, M.J., Sanjuan, J., 2012. Multimodal morphometry and functional magnetic resonance imaging in schizophrenia and auditory hallucinations. *World J. Radiol.* 4, 159–166. <https://doi.org/10.4329/wjr.v4.i4.159>.

Gaser, C., Nenadic, L., Volz, H.-P., Büchel, C., Sauer, H., 2004. Neuroanatomy of 'hearing voices': a frontotemporal brain structural abnormality associated with auditory hallucinations in schizophrenia. *Cereb. Cortex* 14, 91–96.

Glahn, D.C., Laird, A.R., Ellison-Wright, I., Thelen, S.M., Robinson, J.L., Lancaster, J.L., Bullmore, E., Fox, P.T., 2008. Meta-analysis of gray matter anomalies in schizophrenia: application of anatomical likelihood estimation and network analysis. *Biol. Psychiatry* 64, 774–781. <https://doi.org/10.1016/j.biopsych.2008.03.031>.

Goldstein, J.M., Goodman, J.M., Seidman, L.J., Kennedy, D.N., Makris, N., Lee, H., Tourville, J., Caviness Jr., V.S., Faraone, S.V., Tsuang, M.T., 1999. Cortical abnormalities in schizophrenia identified by structural magnetic resonance imaging. *Arch Gen Psychiatry* 56, 537–547. <https://doi.org/10.1001/archpsyc.56.6.537>.

Hanford, L.C., Nizarov, A., Hall, G.B., Sassi, R.B., 2016. Cortical thickness in bipolar disorder: a systematic review. *Bipolar Disord.* 18, 4–18. <https://doi.org/10.1111/bdi.12111>.

- 12362.
- Hergueta, T., Baker, R., Dunbar, G.C., 1998. The Mini-International Neuropsychiatric Interview (MIND): the development and validation of a structured diagnostic psychiatric interview for DSM-IV and ICD-10. *J. Clin. Psychiatry* 59, 2233.
- Hermundstad, A.M., Bassett, D.S., Brown, K.S., Aminoff, E.M., Clewett, D., Freeman, S., Frithsen, A., Johnson, A., Tipper, C.M., Miller, M.B., Grafton, S.T., Carlson, J.M., 2013. Structural foundations of resting-state and task-based functional connectivity in the human brain. *Proc. Natl. Acad. Sci. U. S. A.* 110, 6169–6174. <https://doi.org/10.1073/pnas.1219562110>.
- Hermundstad, A.M., Brown, K.S., Bassett, D.S., Aminoff, E.M., Frithsen, A., Johnson, A., Tipper, C.M., Miller, M.B., Grafton, S.T., Carlson, J.M., 2014. Structurally-constrained relationships between cognitive states in the human brain. *PLoS Comput. Biol.* 10, e1003591. <https://doi.org/10.1371/journal.pcbi.1003591>.
- Holzel, B.K., Carmody, J., Vangel, M., Congleton, C., Yerramsetti, S.M., Gard, T., Lazar, S.W., 2011. Mindfulness practice leads to increases in regional brain gray matter density. *Psychiatry Res* 191, 36–43. <https://doi.org/10.1016/j.psychres.2010.08.006>.
- Hunter, M.A., Takane, Y., 2002. Constrained principal component analysis: various applications. *Journal of Educational and Behavioral Statistics* 27, 105–145.
- Ivleva, E.I., Bidesi, A.S., Keshavan, M.S., Pearlson, G.D., Meda, S.A., Dodig, D., Moates, A.F., Lu, H., Francis, A.N., Tandon, N., 2013. Gray matter volume as an intermediate phenotype for psychosis: bipolar-Schizophrenia Network on Intermediate Phenotypes (B-SNIP). *Am. J. Psychiatry* 170, 1285–1296.
- Jardri, R., Pins, D., Lafargue, G., Very, E., Ameller, A., Delmaire, C., Thomas, P., 2011a. Increased overlap between the brain areas involved in self-other distinction in schizophrenia. *PLoS ONE* 6, e17500.
- Jardri, R., Pouchet, A., Pins, D., Thomas, P., 2011b. Cortical activations during auditory verbal hallucinations in schizophrenia: a coordinate-based meta-analysis. *Am. J. Psychiatry* 168, 73–81. <https://doi.org/10.1176/appi.ajp.2010.09101522>.
- Jardri, R., Thomas, P., Delmaire, C., Delion, P., Pins, D., 2013. The neurodynamic organization of modality-dependent hallucinations. *Cereb Cortex* 23, 1108–1117. <https://doi.org/10.1093/cercor/bhs082>.
- Koch, K., Wagner, G., Schachtzabel, C., Schultz, C.C., Gullmar, D., Reichenbach, J.R., Sauer, H., Schlosser, R.G., 2011. Neural activation and radial diffusivity in schizophrenia: combined fMRI and diffusion tensor imaging study. *Br. J. Psychiatry* 198, 223–229. <https://doi.org/10.1192/bjp.bp.110.081836>.
- Kubera, K.M., Rashidi, M., Schmitgen, M.M., Barth, A., Hirjak, D., Sambataro, F., Calhoun, V.D., Wolf, R.C., 2019. Structure/function interrelationships in patients with schizophrenia who have persistent auditory verbal hallucinations: a multimodal MRI study using parallel ICA. *Progress. Neuro-Psychopharmacology and Biological Psychiatry*.
- Kubera, K.M., Sambataro, F., Vasic, N., Wolf, N.D., Frasch, K., Hirjak, D., Thomann, P.A., Wolf, R.C., 2014. Source-based morphometry of gray matter volume in patients with schizophrenia who have persistent auditory verbal hallucinations. *Prog. Neuropsychopharmacol. Biol. Psychiatry* 50, 102–109.
- Lavigne, K.M., Hofman, S., Ring, A.J., Ryder, A.G., Woodward, T.S., 2013. The personality of meaning in life: associations between dimensions of life meaning and the Big Five. *J. Posit. Psychol.* 8, 34–43.
- Lavigne, K.M., Rapin, L.A., Metz, P.D., Whitman, J.C., Jung, K., Dohen, M., Loevenbruck, H., Woodward, T.S., 2015. Left-dominant temporal-frontal hypercoupling in schizophrenia patients with hallucinations during speech perception. *Schizophr. Bull.* 41, 259–267. <https://doi.org/10.1093/schbul/sbu004>.
- Lavigne, K.M., Woodward, T.S., 2018. Hallucination and speech-specific hypercoupling in frontotemporal auditory and language networks in schizophrenia using combined task-based fMRI data: an f BIRN study. *Hum. Brain Mapp.* 39, 1582–1595.
- Lawrie, S.M., Buechel, C., Whalley, H.C., Frith, C.D., Friston, K.J., Johnstone, E.C., 2002. Reduced frontotemporal functional connectivity in schizophrenia associated with auditory hallucinations. *Biol. Psychiatry* 51, 1008–1011. [https://doi.org/10.1016/s0006-3223\(02\)01316-1](https://doi.org/10.1016/s0006-3223(02)01316-1).
- Lennox, B.R., Park, S.B., Medley, I., Morris, P.G., Jones, P.B., 2000. The functional anatomy of auditory hallucinations in schizophrenia. *Psychiatry Res.* 100, 13–20. [https://doi.org/10.1016/s0925-4927\(00\)00068-8](https://doi.org/10.1016/s0925-4927(00)00068-8).
- Liddle, P.F., Ngan, E.T., Duffield, G., Kho, K., Warren, A.J., 2002. Signs and Symptoms of Psychotic Illness (SSPI): a rating scale. *Br. J. Psychiatry* 180, 45–50. <https://doi.org/10.1192/bjp.180.1.45>.
- Liu, S., Cai, W., Liu, S., Zhang, F., Fulham, M., Feng, D., Pujol, S., Kikinis, R., 2015. Multimodal neuroimaging computing: a review of the applications in neuropsychiatric disorders. *Brain Inform* 2, 167–180. <https://doi.org/10.1007/s40708-015-0019-x>.
- Luk, J., Underhill, K., Woodward, T.S., 2018. Psychotic symptoms predicting evidence integration in schizophrenia. *Zeitschrift für Psychologie*.
- Lyoo, I.K., Sung, Y.H., Dager, S.R., Friedman, S.D., Lee, J.Y., Kim, S.J., Kim, N., Dunner, D.L., Renshaw, P.F., 2006. Regional cerebral cortical thinning in bipolar disorder. *Bipolar Disord* 8, 65–74. <https://doi.org/10.1111/j.1399-5618.2006.00284.x>.
- Manoliu, A., Riedl, V., Zherdin, A., Muhlau, M., Schwerthoff, D., Scherr, M., Peters, H., Zimmer, C., Forstl, H., Bauml, J., Wohlschläger, A.M., Sorg, C., 2014. Aberrant dependence of default mode/central executive network interactions on anterior insular salience network activity in schizophrenia. *Schizophr Bull* 40, 428–437. <https://doi.org/10.1093/schbul/sbt037>.
- Martí-Bonmati, L., Lull, J.J., García-Martí, G., Aguilar, E.J., Moratal-Pérez, D., Poyatos, C., Robles, M., Sanjuán, J., 2007. Chronic auditory hallucinations in schizophrenic patients: MR analysis of the coincidence between functional and morphologic abnormalities. *Radiology* 244, 549–556.
- McGuire, P.K., Silbersweig, D.A., Wright, I., Murray, R.M., David, A.S., Frackowiak, R.S., Frith, C.D., 1995. Abnormal monitoring of inner speech: a physiological basis for auditory hallucinations. *Lancet* 346, 596–600. [https://doi.org/10.1016/s0140-6736\(95\)91435-8](https://doi.org/10.1016/s0140-6736(95)91435-8).
- Metz, P., Feredoes, E., Takane, Y., Wang, L., Weinstein, S., Cairo, T., Ngan, E.T., Woodward, T.S., 2011. Constrained principal component analysis reveals functionally connected load-dependent networks involved in multiple stages of working memory. *Hum. Brain Mapp.* 32, 856–871. <https://doi.org/10.1002/hbm.21072>.
- Metz, P.D., Riley, J.D., Wang, L., Whitman, J.C., Ngan, E.T., Woodward, T.S., 2012. Decreased efficiency of task-positive and task-negative networks during working memory in schizophrenia. *Schizophr Bull* 38, 803–813. <https://doi.org/10.1093/schbul/sbq154>.
- Mitelman, S.A., Canfield, E.L., Newmark, R.E., Brickman, A.M., Torosjan, Y., Chu, K.-W., Hazlett, E.A., Haznedar, M.M., Shihabuddin, L., Buchsbaum, M.S., 2009. Longitudinal assessment of gray and white matter in chronic schizophrenia: a combined diffusion-tensor and structural magnetic resonance imaging study. *Open Neuroimaging J.* 3, 31.
- Modinos, G., Costafreda, S.G., van Tol, M.J., McGuire, P.K., Aleman, A., Allen, P., 2013. Neuroanatomy of auditory verbal hallucinations in schizophrenia: a quantitative meta-analysis of voxel-based morphometry studies. *Cortex* 49, 1046–1055. <https://doi.org/10.1016/j.cortex.2012.01.009>.
- Moorhead, T.W., McKirdy, J., Sussmann, J.E., Hall, J., Lawrie, S.M., Johnstone, E.C., McIntosh, A.M., 2007. Progressive gray matter loss in patients with bipolar disorder. *Biol. Psychiatry* 62, 894–900. <https://doi.org/10.1016/j.biopsych.2007.03.005>.
- Mørch-Johnsen, L., Nesvåg, R., Jørgensen, K.N., Lange, E.H., Hartberg, C.B., Haukvik, U.K., Kompus, K., Westeraasen, R., Osnes, K., Andreassen, O.A., Melle, I., Høgdahl, K., Agartz, I., 2017. Auditory Cortex Characteristics in Schizophrenia: associations With Auditory Hallucinations. *Schizophr. Bull.* 43, 75–83. <https://doi.org/10.1093/schbul/sbw130>.
- Murray, R.M., Sham, P., Van Os, J., Zanelli, J., Cannon, M., McDonald, C., 2004. A developmental model for similarities and dissimilarities between schizophrenia and bipolar disorder. *Schizophr. Res.* 71, 405–416.
- Neckelmann, G., Specht, K., Lund, A., Erslund, L., Smievoll, A.I., Neckelmann, D., Høgdahl, K., 2006. Morphometry analysis of grey matter volume reduction in schizophrenia: association with hallucinations. *Int. J. Neurosci.* 116, 9–23. <https://doi.org/10.1080/00207450690962244>.
- Nenadic, I., Maitra, R., Langbein, K., Dietzek, M., Lorenz, C., Smesny, S., Reichenbach, J.R., Sauer, H., Gaser, C., 2015. Brain structure in schizophrenia vs. psychotic bipolar I disorder: a VBM study. *Schizophr. Res.* 165, 212–219. <https://doi.org/10.1016/j.schres.2015.04.007>.
- Nenadic, I., Smesny, S., Schlosser, R.G., Sauer, H., Gaser, C., 2010. Auditory hallucinations and brain structure in schizophrenia: voxel-based morphometric study. *Br. J. Psychiatry* 196, 412–413. <https://doi.org/10.1192/bjp.bp.109.070441>.
- Padmanabhan, J.L., Tandon, N., Haller, C.S., Mathew, I.T., Eack, S.M., Clementz, B.A., Pearlson, G.D., Sweeney, J.A., Tamminga, C.A., Keshavan, M.S., 2014. Correlations between brain structure and symptom dimensions of psychosis in schizophrenia, schizoaffective, and psychotic bipolar I disorders. *Schizophr. Bull.* 41, 154–162.
- Palaniyappan, L., Balain, V., Radua, J., Liddle, P.F., 2012. Structural correlates of auditory hallucinations in schizophrenia: a meta-analysis. *Schizophr. Res.* 137, 169–173. <https://doi.org/10.1016/j.schres.2012.01.038>.
- Palaniyappan, L., Marques, T.R., Taylor, H., Handley, R., Mondelli, V., Bonaccorso, S., Giordano, A., McQueen, G., DiForti, M., Simmons, A., 2013. Cortical folding defects as markers of poor treatment response in first-episode psychosis. *JAMA Psychiatry* 70, 1031–1040.
- Panizzon, M.S., Fennema-Notestine, C., Eyler, L.T., Jernigan, T.L., Prom-Wormley, E., Neale, M., Jacobson, K., Lyons, M.J., Grant, M.D., Franz, C.E., Xian, H., Tsuang, M., Fischl, B., Seidman, L., Dale, A., Kremen, W.S., 2009. Distinct genetic influences on cortical surface area and cortical thickness. *Cereb Cortex* 19, 2728–2735. <https://doi.org/10.1093/cercor/bhp026>.
- Pynn, L.K., DeSouza, J.F., 2013. The function of efference copy signals: implications for symptoms of schizophrenia. *Vision Res.* 76, 124–133. <https://doi.org/10.1016/j.visres.2012.10.019>.
- Qiu, A., Gan, S.C., Wang, Y., Sim, K., 2013. Amygdala-hippocampal shape and cortical thickness abnormalities in first-episode schizophrenia and mania. *Psychol. Med.* 43, 1353–1363. <https://doi.org/10.1017/S0033291712002218>.
- Rapin, L.A., Dohen, M., Loevenbruck, H., Whitman, J.C., Metz, P.D., Woodward, T.S., 2012. Hyperintensity of functional networks involving voice-selective cortical regions during silent thought in schizophrenia. *Psychiatry Res* 202, 110–117. <https://doi.org/10.1016/j.psychres.2011.12.014>.
- Rimol, L.M., Hartberg, C.B., Nesvåg, R., Fennema-Notestine, C., Hagler Jr., D.J., Pung, C.J., Jennings, R.G., Haukvik, U.K., Lange, E., Nakstad, P.H., Melle, I., Andreassen, O.A., Dale, A.M., Agartz, I., 2010. Cortical thickness and subcortical volumes in schizophrenia and bipolar disorder. *Biol. Psychiatry* 68, 41–50. <https://doi.org/10.1016/j.biopsych.2010.03.036>.
- Rimol, L.M., Nesvåg, R., Hagler Jr., D.J., Bergmann, O., Fennema-Notestine, C., Hartberg, C.B., Haukvik, U.K., Lange, E., Pung, C.J., Server, A., Melle, I., Andreassen, O.A., Agartz, I., Dale, A.M., 2012. Cortical volume, surface area, and thickness in schizophrenia and bipolar disorder. *Biol. Psychiatry* 71, 552–560. <https://doi.org/10.1016/j.biopsych.2011.11.026>.
- Rosen, C., Marvin, R., Reilly, J.L., DeLeon, O., Harris, M.S., Keedy, S.K., Solari, H., Weiden, P., Sweeney, J.A., 2012. Phenomenology of first-episode psychosis in schizophrenia, bipolar disorder, and unipolar depression: a comparative analysis. *Clin. Schizophr. Relat. Psychoses* 6, 145–151. <https://doi.org/10.3371/CSRP.6.3.6>.
- Rosen, L.N., Rosenthal, N.E., Dunner, D.L., Fieve, R.R., 1983. Social outcome compared in psychotic and nonpsychotic bipolar I patients. *J. Nerv. Ment. Dis.* 171, 272–275. <https://doi.org/10.1097/00005053-198305000-00022>.
- Sanjuán, J., Lull, J.J., Aguilar, E.J., Martí-Bonmati, L., Moratal, D., Gonzalez, J.C., Robles, M., Keshavan, M.S., 2007. Emotional words induce enhanced brain activity in schizophrenic patients with auditory hallucinations. *Psychiatry Res.* 154, 21–29. <https://doi.org/10.1016/j.psychres.2006.04.011>.

- Schlosser, R.G., Nenadic, I., Wagner, G., Gullmar, D., von Consbruch, K., Kohler, S., Schultz, C.C., Koch, K., Fitzek, C., Matthews, P.M., Reichenbach, J.R., Sauer, H., 2007. White matter abnormalities and brain activation in schizophrenia: a combined DTI and fMRI study. *Schizophr Res.* 89, 1–11. <https://doi.org/10.1016/j.schres.2006.09.007>.
- Schultz, C.C., Fusar-Poli, P., Wagner, G., Koch, K., Schachtzabel, C., Gruber, O., Sauer, H., Schlosser, R.G., 2012a. Multimodal functional and structural imaging investigations in psychosis research. *Eur. Arch. Psychiatry. Clin. Neurosci.* 262 (Suppl 2), S97–106. <https://doi.org/10.1007/s00406-012-0360-5>.
- Schultz, C.C., Koch, K., Wagner, G., Nenadic, I., Schachtzabel, C., Gullmar, D., Reichenbach, J.R., Sauer, H., Schlösser, R.G., 2012b. Reduced Anterior Cingulate Cognitive Activation Is Associated with Prefrontal–Temporal Cortical Thinning in Schizophrenia. *Biol. Psychiatry* 71, 146–153.
- Seminowicz, D.A., Shpaner, M., Keaser, M.L., Krauthamer, G.M., Mantegna, J., Dumas, J.A., Newhouse, P.A., Filippi, C.G., Keefe, F.J., Naylor, M.R., 2013. Cognitive-behavioral therapy increases prefrontal cortex gray matter in patients with chronic pain. *J. Pain* 14, 1573–1584. <https://doi.org/10.1016/j.jpain.2013.07.020>.
- Shergill, S.S., Brammer, M.J., Fukuda, R., Williams, S.C., Murray, R.M., McGuire, P.K., 2003. Engagement of brain areas implicated in processing inner speech in people with auditory hallucinations. *Br. J. Psychiatry* 182, 525–531. <https://doi.org/10.1192/bjp.182.6.525>.
- Smith, L.M., Johns, L.C., Mitchell, R., 2017. Characterizing the experience of auditory verbal hallucinations and accompanying delusions in individuals with a diagnosis of bipolar disorder: a systematic review. *Bipolar Disord* 19, 417–433. <https://doi.org/10.1111/bdi.12520>.
- Sommer, I.E., Clos, M., Meijering, A.L., Diederer, K.M., Eickhoff, S.B., 2012. Resting state functional connectivity in patients with chronic hallucinations. *PLoS ONE* 7, e43516. <https://doi.org/10.1371/journal.pone.0043516>.
- Spaniel, F., Tintera, J., Rydlo, J., Ibrahim, I., Kasperek, T., Horacek, J., Zaytseva, Y., Matejka, M., Fialova, M., Slovakova, A., Mikolas, P., Melicher, T., Gornerova, N., Hoschl, C., Hajek, T., 2016. Altered Neural Correlate of the Self-Agency Experience in First-Episode Schizophrenia-Spectrum Patients: an fMRI Study. *Schizophr. Bull.* 42, 916–925. <https://doi.org/10.1093/schbul/sbv188>.
- Sprengh, R.N., Mar, R.A., Kim, A.S., 2009. The common neural basis of autobiographical memory, prospection, navigation, theory of mind, and the default mode: a quantitative meta-analysis. *J. Cogn. Neurosci.* 21, 489–510. <https://doi.org/10.1162/jocn.2008.21029>.
- Sui, J., Pearlson, G.D., Du, Y., Yu, Q., Jones, T.R., Chen, J., Jiang, T., Bustillo, J., Calhoun, V.D., 2015. In search of multimodal neuroimaging biomarkers of cognitive deficits in schizophrenia. *Biol. Psychiatry* 78, 794–804. <https://doi.org/10.1016/j.biopsych.2015.02.017>.
- Sui, J., Yu, Q., He, H., Pearlson, G.D., Calhoun, V.D., 2012. A selective review of multimodal fusion methods in schizophrenia. *Front Hum Neurosci.* 6, 27. <https://doi.org/10.3389/fnhum.2012.00027>.
- Supekar, K., Cai, W., Krishnadas, R., Palaniyappan, L., Menon, V., 2019. Dysregulated Brain Dynamics in a Triple-Network Saliency Model of Schizophrenia and Its Relation to Psychosis. *Biol. Psychiatry* 85, 60–69. <https://doi.org/10.1016/j.biopsych.2018.07.020>.
- Takane, Y., Hunter, M.A., 2001. Constrained principal component analysis: a comprehensive theory. *Applicable Algebra in Engineering, Communication and Computing* 12, 391–419.
- Takane, Y., Shibayama, T., 1991. Principal component analysis with external information on both subjects and variables. *Psychometrika* 56, 97–120.
- Van Erp, T.G., Walton, E., Hibar, D.P., Schmaal, L., Jiang, W., Glahn, D.C., Pearlson, G.D., Yao, N., Fukunaga, M., Hashimoto, R., 2018. Cortical brain abnormalities in 4474 individuals with schizophrenia and 5098 control subjects via the Enhancing Neuroimaging Genetics Through Meta Analysis (ENIGMA) Consortium. *Biol. Psychiatry* 84, 644–654.
- van Lutterveld, R., Diederer, K.M., Otte, W.M., Sommer, I.E., 2014. Network analysis of auditory hallucinations in nonpsychotic individuals. *Hum Brain Mapp.* 35, 1436–1445. <https://doi.org/10.1002/hbm.22264>.
- Wang, L., Hosakere, M., Trein, J.C., Miller, A., Ratnanather, J.T., Barch, D.M., Thompson, P.A., Qiu, A., Gado, M.H., Miller, M.I., Csernansky, J.G., 2007. Abnormalities of cingulate gyrus neuroanatomy in schizophrenia. *Schizophr Res.* 93, 66–78. <https://doi.org/10.1016/j.schres.2007.02.021>.
- Waters, F., Allen, P., Aleman, A., Fernyhough, C., Woodward, T.S., Badcock, J.C., Barkus, E., Johns, L., Varese, F., Menon, M., Vercammen, A., Laroi, F., 2012. Auditory hallucinations in schizophrenia and nonschizophrenia populations: a review and integrated model of cognitive mechanisms. *Schizophr. Bull.* 38, 683–693. <https://doi.org/10.1093/schbul/sbs045>.
- Whitfield-Gabrieli, S., Thermenos, H.W., Milanovic, S., Tsuang, M.T., Faraone, S.V., McCarley, R.W., Shenton, M.E., Green, A.I., Nieto-Castanon, A., LaViolette, P., Wojcik, J., Gabrieli, J.D., Seidman, L.J., 2009. Hyperactivity and hyperconnectivity of the default network in schizophrenia and in first-degree relatives of persons with schizophrenia. *Proc. Natl. Acad. Sci. U. S. A.* 106, 1279–1284. <https://doi.org/10.1073/pnas.0809141106>.
- Winkler, A.M., Kochunov, P., Blangero, J., Almasy, L., Zilles, K., Fox, P.T., Duggirala, R., Glahn, D.C., 2010. Cortical thickness or grey matter volume? The importance of selecting the phenotype for imaging genetics studies. *Neuroimage* 53, 1135–1146. <https://doi.org/10.1016/j.neuroimage.2009.12.028>.
- Woodward, T.S., Cairo, T.A., Ruff, C.C., Takane, Y., Hunter, M.A., Ngan, E.T., 2006. Functional connectivity reveals load dependent neural systems underlying encoding and maintenance in verbal working memory. *Neuroscience* 139, 317–325. <https://doi.org/10.1016/j.neuroscience.2005.05.043>.
- Woodward, T.S., Feredoes, E., Metz, P.D., Takane, Y., Manoach, D.S., 2013. Epoch-specific functional networks involved in working memory. *Neuroimage* 65, 529–539. <https://doi.org/10.1016/j.neuroimage.2012.09.070>.
- Woodward, T.S., Menon, M., 2013. Misattribution models (ii): source monitoring in hallucinating schizophrenia subjects. *The Neuroscience of Hallucinations*. Springer, pp. 169–184.
- Woodward, T.S., Tipper, C.M., Leung, A.L., Lavigne, K.M., Sanford, N., Metz, P.D., 2015. Reduced functional connectivity during controlled semantic integration in schizophrenia: a multivariate approach. *Hum Brain Mapp* 36, 2948–2964. <https://doi.org/10.1002/hbm.22820>.
- Wotruba, D., Michels, L., Buechler, R., Metzler, S., Theodoridou, A., Gerstenberg, M., Walitza, S., Kollias, S., Rössler, W., Heekeren, K., 2013. Aberrant coupling within and across the default mode, task-positive, and salience network in subjects at risk for psychosis. *Schizophr Bull.* 40, 1095–1104.
- Young, R.C., Biggs, J.T., Ziegler, V.E., Meyer, D.A., 1978. A rating scale for mania: reliability, validity and sensitivity. *Br J Psychiatry* 133, 429–435. <https://doi.org/10.1192/bjp.133.5.429>.
- Yuksel, C., McCarthy, J., Shinn, A., Pfaff, D.L., Baker, J.T., Heckers, S., Renshaw, P., Ongur, D., 2012. Gray matter volume in schizophrenia and bipolar disorder with psychotic features. *Schizophr Res.* 138, 177–182. <https://doi.org/10.1016/j.schres.2012.03.003>.
- Zhang, Z., Shi, J., Yuan, Y., Hao, G., Yao, Z., Chen, N., 2008. Relationship of auditory verbal hallucinations with cerebral asymmetry in patients with schizophrenia: an event-related fMRI study. *J. Psychiatr. Res.* 42, 477–486. <https://doi.org/10.1016/j.jpsyres.2007.04.003>.